

**Tumor microenvironment remodeling by intratumoral oncolytic vaccinia virus
enhances the efficacy of immune checkpoint blockade**

Hong Jae Chon^{1,2,3}, Won Suk Lee^{1,2}, Hannah Yang^{1,2}, So Jung Kong^{1,2}, Na Keum Lee^{1,2}, Eun Sang Moon⁴, Jiwon Choi⁴, Eun Chun Han², Joo Hoon Kim^{1,2}, Joong Bae Ahn³, Joo Hang Kim¹ and Chan Kim^{1,2}

¹Medical Oncology, CHA Bundang Medical Center, CHA University, Seongnam 13496, Republic of Korea

²Laboratory of Translational Immuno-Oncology, Seongnam 13488, Republic of Korea

³Yonsei Graduate School, Yonsei University College of Medicine, Seoul 03722, Republic of Korea

⁴SillaJen, Inc., Seoul, 07325, Republic of Korea

HJ Chon and WS Lee contributed equally to this article.

Corresponding Author: Chan Kim, Medical Oncology, CHA Bundang Medical Center, 59 Yatap-ro, Bundang-gu, Seongnam, 13496. Telephone: 82-31-881-7588; Fax: 82-31-780-3929; E-mail: chan@cha.ac.kr or larrel80@gmail.com

Running title: Potentiation of immunotherapy by oncolytic vaccinia virus

Keywords: oncolytic virus, vaccinia virus, immune checkpoint inhibitor, combination immunotherapy, tumor microenvironment

Grant Support: Funded by grants from National Research Foundation of Korea (NRF-2016R1C1B2014671 to C.K. and NRF-2016M3A9E8941664 to H.C) and Korean government (MSIP&MOHW) (No. 2015M3D6A1065644 and HI15C3517).

Disclosure of Potential Conflict of Interest: E.S.M is an employee of SillaJen, Inc. and a member of a Board. J.W.C is an employee of SillaJen, Inc. The other authors declare that they have no competing interests. A patent application based on this work has been filed.

Word count: 4985

Number of figures: 6

Statement of Translational Relevance

Cancer immunotherapies, such as immune checkpoint inhibitors (ICIs), have demonstrated potent therapeutic efficacy. However, many cancer patients have immunosuppressive tumors, leading to resistance against immunotherapy and consequently limited therapeutic response. JX-594 (Pexa-vec) is one of the most promising oncolytic virus platforms in clinical development as one of the few oncolytic viruses in phase III clinical trials. Here, we show that a murine version of JX-594 (JX) remodels the tumor microenvironment by facilitating the accumulation of T cells. As a result, poorly immunogenic tumors become sensitive to ICIs, augmenting the immunotherapeutic efficacy. Of note, the triple-combination therapy of JX, α PD-1, and α CTLA-4 maximizes anti-cancer immunity and induces durable regression with improved overall survival. These findings demonstrate the potential of JX in combination with ICIs for improving anti-cancer immune responses.

Abstract

Purpose: Cancer immunotherapy is a potent treatment modality, but its clinical benefit depends on the tumor's immune profile. Here, we employed mJX-594 (JX), a targeted and GM-CSF-armed oncolytic vaccinia virus, as a strategy to remodel the tumor microenvironment (TME) and subsequently increase sensitivity to α PD-1 and/or α CTLA-4 immunotherapy.

Experimental Design: The remodeling of TME was determined using histologic, flow cytometric, and NanoString immune profiling analyses. JX was intratumorally injected into implanted Renca kidney tumors or *MMTV-PyMT* transgenic mouse breast cancers with or without α PD-1 and/or α CTLA-4. Various combination regimens were used to evaluate immunotherapeutic anti-cancer responses.

Results: Intratumoral injection of JX remodeled the TME through dynamic changes in the immune system, as shown by increased tumor-infiltrating T cells and upregulation of immune-related gene signatures. This remodeling induced conversion of a non-inflamed tumor into an inflamed tumor. JX virotherapy led to enhanced abscopal effects in distant tumors, with increased intratumoral infiltration of CD8⁺ T cells. A depletion study revealed that GM-CSF is an indispensable regulator of anti-cancer efficacy of JX. Dual-combination therapy with intratumoral JX and systemic α PD-1 or α CTLA-4 further enhanced the anti-cancer immune response, regardless of various treatment schedules. Of note, triple-combination immunotherapy with JX, α PD-1, and α CTLA-4 elicited the most potent anti-cancer immunity and induced complete tumor regression and long-term overall survival.

Conclusions: Our results show that intratumoral JX treatment induces dramatic remodeling of TME and more potently suppresses cancer progression with immune checkpoint blockades by overcoming resistance to immunotherapy.

Introduction

Cancer immunotherapy with immune checkpoint inhibitors (ICIs) targeting PD-1 or CTLA-4 has demonstrated a potent and durable therapeutic efficacy and emerged as a new weapon in the war on cancer (1-6). However, the clinical efficacy of ICIs is confined to tumors with a T cell-inflamed tumor microenvironment (TME) (7,8). In poorly immunogenic tumors with few tumor-infiltrating lymphocytes (TILs), TME lacks the type I interferon signature and chemokines for T cell recruitment (9,10). Moreover, tumor vasculatures and stromal components may pose a barrier against intratumoral trafficking of T cells and their effector functions on tumor cells (11-13). Therefore, additional therapeutic interventions are required for these non-T cell-inflamed tumors to appropriately remodel the TME to render these tumors more sensitive to ICI treatments (8,14).

Oncolytic viruses have been proposed as a novel class of anti-cancer therapy, and viruses with different backbones and transgenes are currently being evaluated in clinical trials (15-17). Although the success of oncolytic viruses was initially predicted during the past decade based on their faster replication and enhanced oncolytic capability, they are now beginning to be recognized as an immunotherapeutic because the strongest and most durable responses after oncolytic virotherapy are coupled with successful induction of anti-tumor immunity with increased tumor-specific effector and memory T cells (16,18-21). Nonetheless, because the therapeutic efficacy of oncolytic viruses was greatly hindered by immunosuppressive TME, releasing the brakes of the immune system is critical to maximize the immunotherapeutic efficacy of oncolytic viruses (22-25). Therefore, the combination of oncolytic viruses and ICIs is a rational and appealing strategy to overcome poorly immunogenic and immunosuppressive TME.

JX-594 (pexastimogene devacirepvec, Pexa-vec) is an oncolytic vaccinia virus that is engineered to express an immune-activating transgene, GM-CSF, and that has the viral thymidine kinase gene disrupted (26,27). JX-594 showed impressive anti-cancer activity with low toxicity in preclinical and clinical studies. It has become one of the most feasible and promising oncolytic virus platforms in clinical development as one of the few oncolytic viruses in phase III clinical trials (27-30). In addition to its oncolytic and vascular disrupting activity, JX-594 is proposed to exert an *in situ* cancer vaccination effect because it can elicit the adaptive immune response against tumor antigens for selective tumor disruption and subsequent additional tumor antigen release (31,32). Although JX-594 is now in a phase III randomized clinical trial (NCT02562755) in advanced hepatocellular carcinoma (33), few studies have characterized its immune modulatory functions in primary TME as well as distant lesions after JX-594 treatment (34). Moreover, the optimal combination of JX-594 with immunotherapeutics such as ICIs has not yet been pursued and verified.

Here, we comprehensively dissected the dynamic remodeling of TME with a mouse variant of JX-594 (mJX-594, WR.TK⁻mGM-CSF, hereafter referred to as JX) and investigated its immunotherapeutic potential to provide a rational combinatorial strategy with ICIs in poorly immunogenic tumor models.

Materials and Methods

Mice and cell lines

Male BALB/c mice between 6 to 8 weeks of age were purchased from Orient Bio Inc. (Seongnam, Korea), and female *MMTV-PyMT* transgenic mice (FVB/N) were purchased from Jackson Laboratory (ME, USA, #002374). Mice were housed in a specific-pathogen-free animal facility at CHA University (Seongnam, Korea). All animal experiments were approved by the Institutional Animal Care and Use Committee (IACUC, #170025) of CHA University and were carried out in accordance with the approved protocols. The Renca murine renal cancer cell line and the CT26 murine colon cancer cell line were obtained from the American Type Culture Collection (ATCC, VA, USA #CRL-2947) and Korean Cell Line Bank (Seoul, Korea, #80009). The human cancer cell lines, HeLa S3 and U-2 OS were also originally obtained from ATCC (#CCL-2.2 and #HTB-96). These cells were maintained in Roswell Park Memorial Institute (RPMI) 1640 medium or Dulbecco's Modified Eagle Medium (DMEM), each supplemented with 10% fetal bovine serum (FBS) and 1% penicillin/streptomycin, and were incubated at 37°C, 5% CO₂ in an incubator. All cell lines were used within 10 passages, and confirmed to be mycoplasma-free using the MycoAlert Mycoplasma Detection Kit (Lonza, NJ).

Generation and quantification of virus

mJX-594 (JX), provided by SillaJen, Inc. (Seoul, Korea), is a Western Reserve strain of vaccinia virus encoding murine GM-CSF in the vaccinia thymidine kinase gene locus under the control of the p7.5 promoter (35,36). This virus was amplified in HeLa S3 cells prior to purification. In brief, HeLa S3 cells were infected and incubated with recombinant vaccinia

virus for 3 days, collected by centrifugation, then homogenized and centrifuged once more. The virus-containing supernatant was layered onto a 36% sucrose cushion and centrifuged at 32,900 g, and the purified viral pellet was resuspended in 1 mM Tris, pH 9.0. To determine the viral titer, serially diluted virus in serum-free DMEM was applied onto a monolayer of U-2 OS cells for 2 h, and then 1.5% carboxymethylcellulose in DMEM supplemented with 2 % FBS was added. After 72 h, cells were stained with 0.1% crystal violet and plaques were counted.

Tumor models and treatment regimens

Tumors were implanted by subcutaneous injection of 2×10^5 Renca cells into the right flank of wild type BALB/c mice. When tumors reached $>50 \text{ mm}^3$, mice were treated with either PBS or 1×10^7 plaque forming units (pfu) of JX by intratumoral injection every 3 days. For the bilateral tumor model, 2×10^5 Renca cells were implanted subcutaneously into the right flank, and 1×10^5 Renca or CT26 cells were implanted subcutaneously into the left flank 4 days later. For the cell depletion study, antibodies against CD4 (200 μg , clone GK1.5, BioXCell), CD8 (200 μg , clone 53-6.72, BioXCell), or GM-CSF (200 μg , clone MP1-22E9, BioXCell) were intraperitoneally injected along with intratumoral JX treatment. For immune checkpoint blockade, anti-PD-1 (10 mg/kg, clone J43, BioXCell) and/or anti-CTLA-4 (4 mg/kg, clone 9D9, BioXCell) antibodies were injected intraperitoneally, every 3 days depending on the dosing schedule. Tumors were measured every 2 or 3 days using a digital caliper, and tumor volumes were calculated using the modified ellipsoid formula ($1/2 \times (\text{length} \times \text{width}^2)$). On day 50, the surviving mice with complete tumor regression were re-challenged with 2×10^5 Renca or CT26 cells in the left flank and monitored for tumor growth and survival. Mice were euthanized when tumors reached 1.5 cm in diameter or when mice

became moribund. Female *MMTV-PyMT* transgenic mice were purchased from Jackson Laboratory. Starting at 9 weeks after birth, the volume of every palpable tumor nodule (>20 mm³) was measured, and the total volume of all tumors combined was used to calculate the tumor burden per mouse. *MMTV-PyMT* mice were randomized according to their initial tumor burden, and were treated with 4×10^7 pfu of JX with or without anti-PD-1 (10 mg/kg) or anti-CTLA-4 (4 mg/kg) antibodies at the indicated time points. In particular, JX was injected intratumorally (1×10^7 pfu per tumor) in 4 randomly selected palpable tumors. After 4 weeks of treatment, mice were anesthetized and tissues were harvested for further analyses. Analyses for *MMTV-PyMT* was performed as previously described (37,38).

Statistical analysis

Statistical analyses were performed using GraphPad Prism 7.0 software (GraphPad Software, La Jolla, CA) and PASW statistics 18 (SPSS). Values are represented as mean +/-standard error of the mean unless otherwise indicated. Statistical differences between means were tested using unpaired Student's *t*-tests. Survival curves were generated using the Kaplan-Meier method, and statistical differences between curves were analyzed using the log-rank test. The level of statistical significance was set at $p < 0.05$.

Results

JX converts immunosuppressive non-inflamed tumors into inflamed tumors

To determine the immunomodulatory potential of the oncolytic virus JX, we extensively examined temporal changes in TME after single intratumoral injections of JX into the Renca tumors, which are resistant to immune checkpoint inhibitors (39). The tumoral level of JX was already high at day 1, peaking at day 3, but was barely detectable at day 7 after the injection (**Fig. 1A and B**). Conversely, tumor vessel density was markedly reduced between days 1 and 3 but was recovered at day 7 and thereafter after the injection (**Fig. 1A and B; Supplementary Fig. S1B and S1C**), indicating that JX is a potent but transient tumor vessel disruptor. Of note, the population of CD8⁺ cytotoxic T cells within the tumor, which comprise the most critical aspect of anti-cancer immunity, began to increase strikingly at day 5, peaking at day 7, and remaining at a high density at 2 weeks after injection (**Fig. 1A and B**), demonstrating distinct and long-lasting conversion of the non-inflamed tumor into a T cell–inflamed tumor by JX. By comparison, CD11c⁺ dendritic cells (DCs) transiently emerged at day 3 and then decreased in tumors. However, DCs accumulated in draining lymph nodes from day 5 where they interacted with CD8⁺ T cells (**Fig. 1A; Supplementary Fig. S1D**). In addition, the level of PD-L1 was low at day 0 and upregulated after JX treatment (**Fig. 1A and B**). Intriguingly, the PD-L1 upregulation followed just after a massive influx of CD8⁺ TILs (**Fig. 1C**), indicating activation of the PD-1/PD-L1 axis in an attempt to negatively regulate T cell–mediated immunity. Most PD-L1⁺ cells were cytokeratin⁺ tumor cells, and some were CD11b⁺ myeloid but were not T cells (**Fig. 1D**). Thus, JX is not only a transient tumor vessel disruptor but also a potent and durable anti-cancer immunity enhancer. In contrast to JX-treated tumors, control tumors showed no significant changes in CD31⁺ blood

vessels, CD8⁺ cytotoxic T cells, CD11c⁺ DCs, or PD-L1⁺ cells (**Supplementary Fig. S1A**).

To elucidate the cancer immune pathways modulated by JX, we further analyzed changes in expression of 750 immune-related genes in the Renca tumor following JX monotherapy, using a PanCancer Immune Profiling panel. Of note, expression levels of the genes (~100 genes) related to immune modulation, including activation of type I IFN signaling, DC maturation, and T cell activation, were significantly different between control- and JX-treated tumors (**Fig. 1E and F**). In particular, the genes related to inhibitory immune checkpoints (Pd-1, Pd-11, Ctla-4, and Lag-3) and agonistic immune checkpoints (Icos, Gitr, and Cd27), Th1 and Th2 responses, and M1 macrophage polarization (Nos2 and Cd86) were upregulated in JX-treated tumors compared with control-treated tumors (**Fig. 1G**). These results indicate that JX elicits long-term immune activation through dynamic changes in the TME to remodel non-inflamed tumors into T cell–inflamed tumors that can respond to ICIs.

JX augments intratumoral infiltration of CD8⁺ T cells and induces myeloid cell repolarization

JX-induced delay of tumor growth was dose-dependent (**Supplementary Fig. S2A**). In parallel, JX-induced increases in CD8⁺ T cell infiltration in both peritumoral and intratumoral regions were also dose-dependent (**Supplementary Fig. S2B**). Indeed, flow cytometric subset analysis of the lymphoid cell compartment revealed that the JX-induced increase in absolute numbers of intratumoral CD8⁺ and CD4⁺ T cells was dose-dependent (**Supplementary Fig. S2C and S2D**). Although the number of CD4⁺Foxp3⁺CD25⁺ regulatory T cells increased following the triple administration of JX (**Supplementary Fig. S2E**), the ratio of CD8⁺ T cells to regulatory T cells was 5.3-fold higher compared with that of control treatment (**Supplementary Fig. S2E**), implying an overall increase in T cell

effector function in TME by JX treatment. Additionally, the expression of ICOS and granzyme B (GzB), which are co-stimulatory and T cell activation markers, was increased in CD8⁺ T cells following JX treatment (**Supplementary Fig. S2F**). To confirm the presence of tumor-specific T cells that were recruited into the tumor after JX treatment, IFN- γ ELISPOT assays were performed with isolated TILs and splenocytes. The result was a marked increase in IFN- γ -secreting T cells against Renca tumor cells within tumors and spleens of JX-treated mice compared to control mice. This finding indicated the presence of tumor-specific CD8⁺ T cells in tumors as well as in the lymphoid organ (**Supplementary Fig. S2G**). Further subset analysis of the myeloid cell compartment revealed no significant change in CD11b⁺Gr1⁺ myeloid cell fraction in tumors treated with JX (**Supplementary Fig. S2H**). However, the CD11b⁺Ly6G⁻Ly6C⁺ monocytic myeloid cell fraction was increased, while the CD11b⁺Ly6G⁺Ly6C^{int} granulocytic myeloid cell fraction was reduced, indicating polarization of myeloid cells following JX treatment (**Supplementary Fig. S2I**). These findings demonstrate that repeated JX administration enhances anti-cancer immunity, leading to increased infiltration of activated T cells and repolarization of myeloid cells.

Intratumoral injection of JX leads to systemic and cancer-specific immune responses

To determine whether local injection of JX could induce a systemic immune response for regulating non-injected distant tumors, we administered JX into the right-side tumor after implantation of Renca tumor cells into both side flanks. This treatment suppressed the growth of both right and left (opposite, not injected side) Renca tumors (**Fig. 2A**). In line with tumor growth inhibition on both sides, infiltrations of CD8⁺ T cells at intratumoral regions were increased by 7.9- and 5.5-fold in both right and left Renca tumors (**Fig. 2B**), suggesting that local JX virotherapy can activate systemic anti-cancer immunity.

Next, to exclude the possibility of direct viral spread to the distant tumors through systemic circulation after the local virotherapy, we examined the presence of JX in the left, non-injected Renca tumors and found no immune-detective JX in the left tumors (**Supplementary Fig. S3**). This finding indicated that the anti-cancer activity of JX in distant tumors was systemically immune-mediated and not a result of systemic viral spread.

To evaluate whether the observed systemic immune response was tumor-specific, we performed a similar experiment using mice implanted with Renca tumors on the right flank and CT26 tumors on the left flank. Intratumoral treatment of the right, Renca tumor with JX markedly decreased the growth of the injected tumor, while the growth of the left, untreated CT26 tumor was unaffected (**Fig. 2C**). Moreover, the number of CD8⁺ T cells was not changed in CT26 tumors but was highly increased in Renca tumors (**Fig. 2D**), indicating that JX virotherapy induces a tumor-specific CD8⁺ T cell response. Thus, local JX treatment can elicit systemic and tumor-specific anti-cancer immunity with lymphocyte infiltration to distant tumors.

Anti-cancer immunity plays a critical role in the overall therapeutic efficacy of JX

To determine which components of the immune system are responsible for the therapeutic efficacy of JX, we examined its effect on tumors in mice treated with neutralizing antibodies against CD8, CD4, or GM-CSF (**Supplementary Fig. S4A**). Of special note, depletion of either CD8⁺ or CD4⁺ T cells abrogated the effective tumor growth inhibition by JX (**Supplementary Fig. S4B and S4C**), emphasizing the importance of an immune-mediated mechanism rather than direct oncolysis in JX-induced tumor growth inhibition. Intriguingly, depletion of CD4⁺ T cells at the time of JX injection reduced intratumoral infiltration of

CD8⁺ T cell (**Supplementary Fig. S4D**), indicating that CD4⁺ T cells are involved in activation and recruitment of CD8⁺ T cells in TME. However, depletion of CD8⁺ T cells did not significantly alter infiltration of CD4⁺ T cells (**Supplementary Fig. S4D**), indicating that CD8⁺ T cells did not affect CD4⁺ T cells in TME. These findings indicate that intratumoral JX treatment induces priming of CD8⁺ and CD4⁺ T cells, which may interact with each other to mediate anti-cancer immunity.

Previous virotherapy based on herpes and vaccinia viruses used GM-CSF as an immune-activating transgene, which recruits and activates antigen-presenting cells that subsequently trigger T cell response (40). However, the use of GM-CSF is still controversial because of its potential immunosuppressive roles in tumor progression, such as inducing proliferation of myeloid-derived suppressor cells (18). Therefore, we explored whether GM-CSF is required for the therapeutic effect of JX. Interestingly, depletion of GM-CSF negated the anti-tumor effect of JX and reduced both CD8⁺ and CD4⁺ T cell levels, suggesting that GM-CSF is critical for the immunotherapeutic efficacy of JX (**Supplementary Fig. S4C and S4D**). Thus, both CD8⁺ and CD4⁺ T cells are indispensable mediators of the anti-cancer effect of JX, and GM-CSF is an essential regulator of T cell activation for the JX treatment.

Combination of JX with immune checkpoint blockade elicits an enhanced anti-cancer effect with augmented infiltration of T lymphocytes into the tumor

As shown earlier, while JX inflames the TME by enhancing the recruitment of CD8⁺ T cells, it concomitantly increases the expression of PD-L1, which hinders the anti-cancer effects of cytotoxic T cells. On the other hand, ICI monotherapy is ineffective in non-inflamed, T cell-insufficient tumors (8). Therefore, we sought to combine the two modalities to compensate for their respective weaknesses.

The combination of anti-PD-1 antibody (α PD-1) and JX reduced tumor growth by 70%, while α PD-1 and JX monotherapy delayed tumor growth by 23% and 44%, respectively (**Fig. 3A**). In support of these findings, CD8⁺ T cells were more highly infiltrated in both peritumoral (2.5-fold) and intratumoral (2.4-fold) regions of the tumors treated with combination therapy than those treated with JX (**Fig. 3B and C**). Furthermore, CD31⁺ tumor blood vessels were decreased by combination therapy compared to control (peritumoral and intratumoral regions, 1.8-fold and 2.6-fold, respectively; **Fig. 3B and C; Supplementary Fig. S5A**), and tumor apoptosis was most severely induced in tumors treated with combination therapy compared with all other groups (**Fig. 3B and C; Supplementary Fig. S5B**). Similarly to our initial findings (**Fig. 1A–C**), although the PD-L1 expression was minimal in control tumors, it was upregulated by 2.1~3.7 fold in both peritumoral and intratumoral regions of JX-treated tumors (**Fig. 3B and C; Supplementary Fig. S5B**), implying that PD-L1 involves an adaptive negative feedback mechanism that dampens anti-cancer immunity after oncolytic virotherapy.

Next, to determine whether combination therapy is effective against distant untreated tumors as well as injected tumors, we treated mice carrying bilateral Renca tumors with JX and/or α PD-1 (**Supplementary Fig. S5C**). The combination therapy more potently suppressed the growth of distant untreated tumors compared to JX or α PD-1 monotherapy.

Therefore, our findings indicate that combining JX and ICI not only potentiates the systemic immunotherapeutic effect of JX virotherapy but also overcomes resistance against ICI monotherapy through enhanced anti-cancer immunity by increasing CD8⁺ T cell infiltration (**Fig. 3D**).

We further validated our hypothesis by testing the efficacy of combination treatment with anti-CTLA-4 antibody (α CTLA-4) and JX. Although tumor growth was modestly inhibited by either JX (42.0%) or α CTLA-4 (20.0%) monotherapy, combination therapy displayed the most potent inhibitory effect (57.6%) (**Supplementary Fig. S6A**). In addition, CD8⁺ T cells were more highly accumulated in both peritumoral (1.9-fold increase) and intratumoral (1.9-fold increase) regions of tumors treated with combination therapy compared with JX (**Supplementary Fig. S6B and S6C**). CD31⁺ tumor blood vessels were also disrupted in both peritumoral and intratumoral regions of combination therapy–treated tumors compared with control (2.1-fold and 3.8-fold reductions, respectively; **Supplementary Fig. S6B and S6C**). Furthermore, flow cytometry revealed that intratumoral infiltration of CD8⁺ and CD4⁺ T cells was also increased by JX and α CTLA-4 combination therapy (**Supplementary Fig. S6D**). Taken together, these results indicate that combination therapy using JX and ICIs can overcome the resistance against immunotherapy in immunosuppressive TMEs, resulting in enhanced anti-cancer effects.

The efficacy of combination immunotherapy with intratumoral JX and ICIs is not largely affected by treatment schedule

Because ICIs can negatively affect viral replication and lead to premature clearance of the oncolytic virus, previous studies explored the optimal schedules of treatment using combinations of systemic oncolytic virotherapy and ICIs and reported that some combination schedules could antagonize the therapeutic efficacy (22,41). However, the dependency of local oncolytic virotherapy on the treatment schedule of ICIs has not been reported. To establish the optimal combination schedule for intratumoral JX and ICIs, we compared the following: (1) simultaneous administration of JX and ICI (schedule I); (2) initiation of ICI 3

days after administration of JX (schedule II); and (3) administration of JX 3 days after initiation of ICI (schedule III) (**Fig. 4A**). All combination schedules delayed tumor growth by ~40% (**Fig. 4B**). Likewise, levels of tumor-infiltrating CD8⁺ and CD4⁺ T cells were increased by >8.0-fold and >4.0-fold, respectively, and the expression of ICOS and GzB in CD8⁺ T cells was remarkably increased compared to control regardless of treatment schedule (**Fig. 4C and D**).

Similar to combination therapy with JX and α PD-1, the combination of JX and α CTLA-4 inhibited tumor growth by ~40% regardless of the treatment schedule (**Supplementary Fig. S7A**). Furthermore, intratumoral infiltration of CD8⁺ and CD4⁺ T lymphocytes (>7-fold and >7-fold increases, respectively) and GzB and ICOS expression in CD8⁺ T cells were greater regardless of treatment schedule (**Supplementary Fig. S7B and S7C**).

The therapeutic efficacy of concurrent combination therapy with ICIs and oncolytic viruses varies depending on the virus administration route because viral clearance by adaptive immunity may differ when the oncolytic virus is injected either systemically (intravenous) or locally (intratumoral) (22,41). Therefore, we hypothesized that the administration route could affect the efficacy of concurrent combination therapy. To test this hypothesis, we compared intravenous versus intratumoral injection of JX concurrently with α PD-1 (**Supplementary Fig. S8A and S8B**). Intriguingly, in tumors treated with intravenous JX, JX tumoral levels were remarkably reduced with concurrent α PD-1 treatment. In contrast, in tumors treated with intratumoral JX, concurrent α PD-1 treatment had almost no effect on tumoral levels of JX. Therefore, concurrent α PD-1 treatment seems less likely to affect JX if JX is administered via intratumoral injection.

Collectively, combination therapy with intratumoral JX injection and systemic ICI led to an effective anti-cancer immunity regardless of treatment schedule, suggesting that intratumoral

administration of JX could minimize the potential antagonism with systemic ICI treatment.

Triple combination of JX, α PD-1, and α CTLA-4 induces profound tumor regression and provides a long-term survival benefit in implanted kidney cancer

As dual combination of JX and ICIs did not induce complete tumor regression, we explored the effect of triple combination therapy using JX, α PD-1, and α CTLA-4. While the dual combination of α PD-1 and α CTLA-4 delayed tumor growth by 14.5% and JX monotherapy inhibited tumor growth by 36.9%, the triple combination inhibited tumor growth by 76.5% (**Fig. 5A**). Of note, a few mice (~40%) of this triple combination group exhibited complete tumor regression, which was not observed in any other groups (**Fig. 5B**). Furthermore, mice with complete tumor regression were tumor-free for more than 14 weeks after treatment cessation. They also were fully protected against re-challenge with Renca tumor cells but were not immune to CT26 tumor cells, suggesting the establishment of an effective, long-term, and tumor-specific immune memory (**Fig. 5C**).

To establish that the potent anti-cancer effects induced by triple combination therapy could translate into a long-term survival benefit, we performed survival analyses of tumor-bearing mice (**Fig. 5D**). Mice treated with triple-combination immunotherapy showed a remarkably better overall survival compared to results with monotherapy or dual-combination therapy. Intriguingly, the difference between dual and triple combination therapy was not remarkable early in the treatment period, but it increased over time and was maintained for a long time. Therefore, triple combination therapy is needed to induce durable immunotherapeutic effects and longer survival. In conclusion, these findings demonstrate that triple combination immunotherapy has the potential to induce complete tumor regression and long-term survival.

The triple combination therapy enhances anti-cancer immune responses in a spontaneous breast cancer model

To validate the long-term immunotherapeutic efficacy of the triple combination therapy in immune-resistant tumors, we employed the *MMTV-PyMT* transgenic mouse model, which is a spontaneous breast cancer model with intrinsic resistance to immune checkpoint blockade (42). After 4 weeks of treatment, mice treated with the triple combination of JX, α PD-1, and α CTLA-4 exhibited a significant reduction in overall tumor burden by 48.1% and a delay in the development of palpable tumor nodules compared with control mice (**Fig. 6A–D**). Furthermore, triple-combination therapy led to a 48.1% reduction in average tumor nodule size and better overall survival compared to other treatments (**Fig. 6E and F**). Histological analyses revealed less invasive carcinoma with well-preserved tumor margins in the triple combination group, indicating that triple combination effectively delays tumor progression and invasion (**Fig. 6G**). Moreover, intratumoral recruitment of CD8⁺ T cells was further increased by 2.0-fold in tumors treated with triple combination therapy compared with those treated with JX monotherapy (**Fig. 6H**). However, tumor vascular density was similar among the treatment groups (**Fig. 6H**), indicating that the vascular disrupting effect is not long-lasting after repeated JX injections. Finally, the number of hematogenous lung metastases was significantly reduced in the triple combination group (**Fig. 6I**), indicating an effective anti-metastatic action by the triple combination therapy. Taken together, these results demonstrated that triple combination immunotherapy with JX and ICIs can elicit a robust anti-cancer immune response even in a poorly immunogenic spontaneous breast cancer model.

Discussion

Here, we demonstrate that combination therapy with JX and ICIs is an effective therapeutic strategy for immune-resistant tumors. The combination therapy leads to an immunological “boiling point” in which a cold, non-inflamed tumor is sufficiently inflamed to enable the host immune system to eradicate tumor cells. The most profound effect was observed with triple immunotherapy with JX, α PD-1, and α CTLA4, which induced complete regression in ~40% of Renca tumors, one of the most resistant syngeneic tumors to immunotherapy. This strong efficacy can be explained by the mutually complementary cooperation of oncolytic virus and ICIs.

JX-594 is an oncolytic virus in the most advanced stage of clinical trials and acts through various mechanisms (27,32,33). Although it can rapidly induce direct oncolysis and vascular disruption in tumors, these effects are transient and mostly diminish within one week of injection. Thereafter, CD8⁺ T cells extensively infiltrate the tumor to initiate anti-cancer immune responses. However, at the same time, tumors begin to evolve to avoid immune-mediated elimination by upregulating immune inhibitory checkpoint molecules such as PD-1, PD-L1, or CTLA-4 in the TME. Because the most potent and durable anti-cancer effects of an oncolytic virus are achieved when it is coupled with successful induction and maintenance of anti-tumor immunity, it is reasonable to combine ICIs with oncolytic virus to prevent early shutdown of oncolytic virotherapy–induced anti-cancer immunity (18).

Although ICI monotherapy revolutionized the treatment landscape of cancer, its dramatic therapeutic response is confined to a subset of patients (1,43). This outcome gave rise to the concept of immunologically ‘hot’ or ‘cold’ tumors: hot tumors respond well to ICIs because they are immunologically inflamed with TILs and show high expression of PD-L1, while

cold tumors are refractory to ICIs because of the paucity of CD8⁺ TILs and immunosuppressive TME (9,24). Therefore, current efforts are focused on overcoming resistance to ICIs by converting immunologically cold tumor to hot tumors. In this respect, our result identifies JX as an ideal combination partner for ICIs. It can selectively replicate in tumor cells, destroy them, and release tumor antigens to stimulate the host immune system. Moreover, our study shows that JX can dramatically convert the TME from a cold to hot state by inducing intratumoral inflammatory responses: induction of Th1 responses along with activation and recruitment of T cells, upregulation of PD-L1, and polarization of myeloid cells toward M1. Intriguingly, the replication and spread of oncolytic viruses is more active in cold tumors where there are few immune cells to eliminate the virus, whereas hot tumors with ample resident TILs can induce premature clearance of virus and attenuate its therapeutic effects (24). Therefore, together with the results of this study, JX emerges as an optimal combination partner for ICIs, especially for non-inflamed cold tumors with intrinsic resistance to immunotherapy.

GM-CSF is the most commonly used therapeutic genetic payload of oncolytic viruses (18,44,45). Two oncolytic viruses in the most advanced phases of clinical trials, T-Vec and Pexa-Vec (JX-594), are both armed with GM-CSF (46). Although GM-CSF is generally known to induce proliferation of various immune cells such as DCs, there is a concern regarding unwanted proliferation of immunosuppressive cells such as myeloid-derived suppressor cells (23,47). In the present study, we revealed that JX did not significantly alter the fraction of intratumoral CD11b⁺Gr1⁺ cells. In addition, neutralization of GM-CSF ablated the therapeutic efficacy of JX, which was partly because of the reduction in CD8⁺ and CD4⁺ TILs, indicating that GM-CSF has an indispensable role in anti-cancer immunity elicited by JX.

Previous studies have reported that although the combination of an oncolytic virus and ICIs elicits an impressive immune response, the therapeutic efficacy can be affected by administration route and treatment schedule (22,41,48). In particular, when both the oncolytic virus and ICIs are systemically administered simultaneously, the combination could be antagonistic because of the ICI-induced anti-viral immunity that can facilitate premature viral clearance, indicating the importance of an adequate time gap in between treatments for the oncolytic virus to induce a successful anti-cancer immunity (41,49). In the present study, local injection of JX consistently induced anti-cancer immunity without being significantly affected by administration sequences. We presume that this result is attributable to the intratumoral injection having provided the oncolytic virus a sufficient time lag to inflame the TME before being detected and eliminated by systemic antiviral immunity. Indeed, in tumors treated with intratumoral JX, concurrent α PD-1 treatment had almost no effect on the tumoral level of JX, in contrast to the markedly decreased level of JX in tumors treated with intravenous JX. Therefore, intratumoral virotherapy may be more suitable for designing clinical trials with the ICI and oncolytic virus combination compared with systemic virotherapy in terms of administration schedule.

In this study, we were not able to exclude the possibility that the immunogenicity of mouse model was affected by a tumor implantation-induced inflammatory reaction (50). While we performed every treatment 10 or 12 days after tumor implantation to minimize inflammatory reaction, the level of the response to treatment that we observed in this study may not fully reflect the immune reaction in human cancer. Therefore, the findings of this preclinical study should be confirmed in clinical trials.

Several clinical trials are ongoing to investigate the efficacy of JX-594 in combination with α PD-1, α CTLA-4, or α PD-L1 to target various solid cancers, including liver, kidney, and

colon cancer (ClinicalTrials.gov: NCT03071094, NCT02977156, NCT03294083, and NCT03206073). Thus, we will be able to verify the findings of this study in a clinical setting in the near future.

In conclusion, these results indicate that intratumoral injection of JX induces a profound remodeling of TME from cold to hot state and elicits robust anti-cancer immunity in combination with ICIs, overcoming immunotherapy resistance.

Author contributions

- Conception and design: Hong Jae Chon, Won Suk Lee, Chan Kim
- Development of methodology: Hong Jae Chon, Won Suk Lee, Chan Kim
- Acquisition of data (provided animals, acquired and managed patients, provided facilities, etc.): Hong Jae Chon, Won Suk Lee, Hannah Yang, So Jung Kong, Na Keum Lee, Chan Kim
- Analysis and interpretation of data (e.g., statistical analysis, biostatistics, computational analysis): Hong Jae Chon, Won Suk Lee, Hannah Yang, Chan Kim
- Writing, review, and/or revision of the manuscript: Hong Jae Chon, Won Suk Lee, Chan Kim
- Administrative, technical, or material support (i.e., reporting or organizing data, constructing databases): Hong Jae Chon, Eun Sang Moon, Jiwon Choi, Eun Chun Han, Joo Hoon Kim, Joong Bae Ahn, Joo Hang Kim, Chan Kim
- Study supervision: Chan Kim

Acknowledgements

This study was supported by the National Research Foundation of Korea (NRF-2016R1C1B2014671 to C. Kim) grant funded by the Ministry of Science, ICT & Future Planning, and by the Bio & Medical Technology Development Program of the National Research Foundation (NRF-2016M3A9E8941664 to H. Chon). This study was also co-supported by the Global High-tech Biomedicine Technology Development Program of the National Research Foundation (NRF) & Korea Health Industry Development Institute (KHIDI) funded by the Korean government (MSIP&MOHW) (No. 2015M3D6A1065644 and HI15C3517).

References

1. Topalian SL, Drake CG, Pardoll DM. Immune checkpoint blockade: a common denominator approach to cancer therapy. *Cancer Cell* **2015**;27(4):450-61.
2. Hegde PS, Karanikas V, Evers S. The Where, the When, and the How of Immune Monitoring for Cancer Immunotherapies in the Era of Checkpoint Inhibition. *Clin. Cancer Res.* **2016**;22(8):1865-74.
3. Wolchok JD, Chan TA. Cancer: Antitumour immunity gets a boost. *Nature* **2014**;515(7528):496-8.
4. Ilett E, Kottke T, Thompson J, Rajani K, Zaidi S, Evgin L, *et al.* Prime-boost using separate oncolytic viruses in combination with checkpoint blockade improves anti-tumour therapy. *Gene Ther.* **2017**;24(1):21-30.
5. Rajani K, Parrish C, Kottke T, Thompson J, Zaidi S, Ilett L, *et al.* Combination Therapy With Reovirus and Anti-PD-1 Blockade Controls Tumor Growth Through Innate and Adaptive Immune Responses. *Mol. Ther.* **2016**;24(1):166-74.
6. Jung HI, Jeong D, Ji S, Ahn TS, Bae SH, Chin S, *et al.* Overexpression of PD-L1 and PD-L2 Is Associated with Poor Prognosis in Patients with Hepatocellular Carcinoma. *Cancer Res. Treat.* **2017**;49(1):246-54.
7. Topalian SL, Taube JM, Anders RA, Pardoll DM. Mechanism-driven biomarkers to guide immune checkpoint blockade in cancer therapy. *Nat. Rev. Cancer* **2016**;16(5):275-87.
8. Gajewski TF. The Next Hurdle in Cancer Immunotherapy: Overcoming the Non-T-Cell-Inflamed Tumor Microenvironment. *Semin. Oncol.* **2015**;42(4):663-71.
9. Gajewski TF, Schreiber H, Fu YX. Innate and adaptive immune cells in the tumor

- microenvironment. *Nat. Immunol.* **2013**;14(10):1014-22.
10. Lechner MG, Karimi SS, Barry-Holson K, Angell TE, Murphy KA, Church CH, *et al.* Immunogenicity of murine solid tumor models as a defining feature of in vivo behavior and response to immunotherapy. *J. Immunother.* **2013**;36(9):477-89.
 11. De Palma M, Jain RK. CD4+ T cell activation and vascular normalization: Two sides of the same coin? *Immunity* **2017**;46(5):773-5.
 12. Rivera LB, Bergers G. Intertwined regulation of angiogenesis and immunity by myeloid cells. *Trends Immunol.* **2015**;36(4):240-9.
 13. Allen E, Jabouille A, Rivera LB, Lodewijckx I, Missiaen R, Steri V, *et al.* Combined antiangiogenic and anti-PD-L1 therapy stimulates tumor immunity through HEV formation. *Sci. Transl. Med.* **2017**;9(385):eaak9679.
 14. Palucka AK, Coussens LM. The basis of oncoimmunology. *Cell* **2016**;164(6):1233-47.
 15. Lichty BD, Breitbach CJ, Stojdl DF, Bell JC. Going viral with cancer immunotherapy. *Nat. Rev. Cancer* **2014**;14(8):559-67.
 16. Bell J. Oncolytic viruses: immune or cytolytic therapy? *Mol. Ther.* **2014**;22(7):1231-2.
 17. Russell SJ, Barber GN. Oncolytic Viruses as Antigen-Agnostic Cancer Vaccines. *Cancer Cell* **2018**;33(4):599-605.
 18. Thorne SH. Immunotherapeutic potential of oncolytic vaccinia virus. *Front. Oncol.* **2014**;4:155.
 19. Chiocca EA, Rabkin SD. Oncolytic viruses and their application to cancer immunotherapy. *Cancer Immunol. Res.* **2014**;2(4):295-300.
 20. Hardcastle J, Mills L, Malo CS, Jin F, Kurokawa C, Geekiyanage H, *et al.* Immunovirotherapy with measles virus strains in combination with anti-PD-1 antibody blockade enhances antitumor activity in glioblastoma treatment. *Neuro.*

- Oncol. **2017**;19(4):493-502.
21. Chen CY, Wang PY, Hutzen B, Sprague L, Swain HM, Love JK, *et al.* Cooperation of Oncolytic Herpes Virotherapy and PD-1 Blockade in Murine Rhabdomyosarcoma Models. *Sci. Rep.* **2017**;7(1):2396.
 22. Liu Z, Ravindranathan R, Kalinski P, Guo ZS, Bartlett DL. Rational combination of oncolytic vaccinia virus and PD-L1 blockade works synergistically to enhance therapeutic efficacy. *Nat. Commun.* **2017**;8:14754.
 23. Hou W, Sampath P, Rojas JJ, Thorne SH. Oncolytic Virus-Mediated Targeting of PGE2 in the Tumor Alters the Immune Status and Sensitizes Established and Resistant Tumors to Immunotherapy. *Cancer Cell* **2016**;30(1):108-19.
 24. Bell JC, Ilkow CS. A viro-immunotherapy triple play for the treatment of glioblastoma. *Cancer Cell* **2017**;32(2):133-4.
 25. Zamarin D, Ricca JM, Sadekova S, Oseledchik A, Yu Y, Blumenschein WM, *et al.* PD-L1 in tumor microenvironment mediates resistance to oncolytic immunotherapy. *J. Clin. Invest.* **2018**;128(4):1413-28.
 26. Kirn DH, Thorne SH. Targeted and armed oncolytic poxviruses: a novel multi-mechanistic therapeutic class for cancer. *Nat. Rev. Cancer* **2009**;9(1):64-71.
 27. Heo J, Reid T, Ruo L, Breitbach CJ, Rose S, Bloomston M, *et al.* Randomized dose-finding clinical trial of oncolytic immunotherapeutic vaccinia JX-594 in liver cancer. *Nat. Med.* **2013**;19(3):329-36.
 28. Cripe TP, Ngo MC, Geller JJ, Louis CU, Currier MA, Racadio JM, *et al.* Phase 1 study of intratumoral Pexa-Vec (JX-594), an oncolytic and immunotherapeutic vaccinia virus, in pediatric cancer patients. *Mol. Ther.* **2015**;23(3):602-8.
 29. Park BH, Hwang T, Liu TC, Sze DY, Kim JS, Kwon HC, *et al.* Use of a targeted

- oncolytic poxvirus, JX-594, in patients with refractory primary or metastatic liver cancer: a phase I trial. *Lancet Oncol.* **2008**;9(6):533-42.
30. Breitbach CJ, Burke J, Jonker D, Stephenson J, Haas AR, Chow LQ, *et al.* Intravenous delivery of a multi-mechanistic cancer-targeted oncolytic poxvirus in humans. *Nature* **2011**;477(7362):99-102.
 31. Breitbach CJ, De Silva NS, Falls TJ, Aladl U, Evgin L, Paterson J, *et al.* Targeting tumor vasculature with an oncolytic virus. *Mol. Ther.* **2011**;19(5):886-94.
 32. Breitbach CJ, Parato K, Burke J, Hwang T-H, Bell JC, Kim DH. Pexa-Vec double agent engineered vaccinia: oncolytic and active immunotherapeutic. *Curr. Opin Virol.* **2015**;13:49-54.
 33. Abou-Alfa GK, Galle PR, Chao Y, Brown KT, Heo J, Borad MJ, *et al.* PHOCUS: A phase 3 randomized, open-label study comparing the oncolytic immunotherapy Pexa-Vec followed by sorafenib (SOR) vs SOR in patients with advanced hepatocellular carcinoma (HCC) without prior systemic therapy. 2016 ASCO Annual Meeting 2016.
 34. Kim M, Nitschké M, Sennino B, Murer P, Schriver BJ, Bell A, *et al.* Amplification of oncolytic vaccinia virus widespread tumor cell killing by sunitinib through multiple mechanisms. *Cancer Res.* **2018**;78(4):922-37.
 35. Breitbach CJ, Arulanandam R, De Silva N, Thorne SH, Patt R, Daneshmand M, *et al.* Oncolytic vaccinia virus disrupts tumor-associated vasculature in humans. *Cancer Res.* **2013**;73(4):1265-75.
 36. Lun X, Chan J, Zhou H, Sun B, Kelly JJ, Stechishin OO, *et al.* Efficacy and safety/toxicity study of recombinant vaccinia virus JX-594 in two immunocompetent animal models of glioma. *Mol. Ther.* **2010**;18(11):1927-36.
 37. Kim C, Yang H, Fukushima Y, Saw PE, Lee J, Park J-S, *et al.* Vascular RhoJ is an

- effective and selective target for tumor angiogenesis and vascular disruption. *Cancer Cell* **2014**;25(1):102-17.
38. Park J-S, Kim I-K, Han S, Park I, Kim C, Bae J, *et al.* Normalization of tumor vessels by Tie2 activation and Ang2 inhibition enhances drug delivery and produces a favorable tumor microenvironment. *Cancer Cell* **2016**;30(6):953-67.
39. Mosely SIS, Prime JE, Sainson RCA, Koopmann J-O, Wang DYQ, Greenawalt DM, *et al.* Rational Selection of Syngeneic Preclinical Tumor Models for Immunotherapeutic Drug Discovery. *Cancer Immunol. Res.* **2017**;5(1):29-41.
40. Thorne SH. The role of GM-CSF in enhancing immunotherapy of cancer. *Immunotherapy* **2013**;5(8):817-9.
41. Rojas JJ, Sampath P, Hou W, Thorne SH. Defining Effective Combinations of Immune Checkpoint Blockade and Oncolytic Virotherapy. *Clin. Cancer Res.* **2015**;21(24):5543-51.
42. Schmittnaegel M, Rigamonti N, Kadioglu E, Cassarà A, Rmili CW, Kiialainen A, *et al.* Dual angiopoietin-2 and VEGFA inhibition elicits antitumor immunity that is enhanced by PD-1 checkpoint blockade. *Sci. Transl. Med.* **2017**;9(385):eaak9670.
43. Sharma P, Allison JP. The future of immune checkpoint therapy. *Science* **2015**;348(6230):56-61.
44. Fukuhara H, Ino Y, Todo T. Oncolytic virus therapy: a new era of cancer treatment at dawn. *Cancer Sci.* **2016**;107(10):1373-9.
45. Hwang T-H, Moon A, Burke J, Ribas A, Stephenson J, Breitbach CJ, *et al.* A mechanistic proof-of-concept clinical trial with JX-594, a targeted multi-mechanistic oncolytic poxvirus, in patients with metastatic melanoma. *Mol. Ther.* **2011**;19(10):1913-22.

46. Sampath P, Thorne SH. Novel therapeutic strategies in human malignancy: combining immunotherapy and oncolytic virotherapy. *Oncolytic Virother.* **2015**;4:75-82.
47. Kohanbash G, McKaveney K, Sakaki M, Ueda R, Mintz AH, Amankulor N, *et al.* GM-CSF promotes the immunosuppressive activity of glioma-infiltrating myeloid cells through interleukin-4 receptor- α . *Cancer Res.* **2013**;73(21):6413-23.
48. Zamarin D, Holmgaard RB, Ricca J, Plitt T, Palese P, Sharma P, *et al.* Intratumoral modulation of the inducible co-stimulator ICOS by recombinant oncolytic virus promotes systemic anti-tumour immunity. *Nat. Commun.* **2017**;8:14340.
49. Fend L, Yamazaki T, Remy C, Fahrner C, Gantzer M, Nourtier V, *et al.* Immune Checkpoint Blockade, Immunogenic Chemotherapy or IFN-alpha Blockade Boost the Local and Abscopal Effects of Oncolytic Virotherapy. *Cancer Res.* **2017**;77(15):4146-57.
50. Jablonska J, Leschner S, Westphal K, Lienenklaus S, Weiss S. Neutrophils responsive to endogenous IFN-beta regulate tumor angiogenesis and growth in a mouse tumor model. *J. Clin. Invest.* **2010**;120(4):1151-64.

Figure legends

Figure 1. JX converts immunosuppressive non-inflamed tumors into inflamed tumors.

Renca tumors were implanted subcutaneously (s.c.) into BALB/c mice and treated with a single intratumoral injection of 1×10^7 plaque-forming units (pfu) of mJX-594 (JX) when tumors reached $>50 \text{ mm}^3$.

(A) Representative images of Renca tumors treated with JX. Tumors sections were stained for JX, CD31, CD8, CD11c, and PD-L1.

(B) Quantifications of JX⁺ area, CD31⁺ blood vessels, CD8⁺ cytotoxic T cells, CD11c⁺ dendritic cells, and PD-L1⁺ cells. * $p < 0.05$ versus day 0.

(C) Temporal changes in JX, CD8, and PD-L1 in tumor microenvironment (TME) after JX treatment.

(D) Images showing upregulated PD-L1 expression (red) in various cell types (green) within the TME after JX treatment. Note that the expression of PD-L1 was mainly observed in Pan-CK⁺ tumor cells (arrowheads), and some CD11b⁺ myeloid cells (arrow) also occasionally expressed PD-L1, while CD3⁺ T cells did not.

(E) NanoString immune-related gene expression heat map. Red and green color represent up- and down-regulated genes, respectively.

(F) Volcano plot showing changes in immune-related gene expressions in JX-treated tumors. Red line indicates $p < 0.05$.

(G) Comparisons of gene expressions related to inhibitory immune checkpoints (ICs), agonistic ICs, Th1 response, Th2 response, TME, and myeloid cell.

Pooled data from two experiments with 5 animals per group. Values are mean \pm SEM. * $p < 0.05$ versus control. Two-tailed Student's *t*-test was used. Scale bars, 50 μm .

Figure 2. Intratumoral injection of JX leads to systemic and cancer-specific immune responses.

Mice were s.c. injected with Renca tumor cells in the right flank and with Renca or CT26 tumors in the left flank. Arrows indicated intratumoral JX treatment.

(A) Growth curves of JX-injected Renca tumor and non-injected Renca tumor.

(B) Representative images and comparisons of CD8⁺ T cells in the JX-injected and non-injected tumors.

(C) Growth curve of JX-injected Renca tumor and non-injected CT26 tumor.

(D) Representative images and comparisons of CD8⁺ T cells in the JX-injected and non-injected tumors.

Unless otherwise denoted, n = 5 for each group. Values are mean ± SD. *p < 0.05 versus control. ns, not significant. Two-tailed Student's *t*-test was used. Scale bars, 50 μm

Figure 3. Combination of JX with α PD-1 elicits an enhanced anti-cancer effect with augmented infiltration of T lymphocytes into the tumor.

Renca tumor-bearing mice were treated with or without JX and α PD-1 on the indicated days (arrows).

(A) Comparisons of tumor growth. Mean and individual tumor growth curves over time.

(B and C) Representative images (B) and comparisons (C) of CD8⁺ T cells, CD31⁺ blood vessels, activated caspase3 (Casp3)⁺ apoptotic cells, and PD-L1⁺ cells in the peri- and intratumoral regions.

(D) Diagram depicting the mechanism by which the immunosuppressive TME is overcome by a combination therapy of JX and immune checkpoint inhibitor (ICI).

Pooled data from two experiments with 7 animals per group. Values are mean \pm SEM. * $p < 0.05$ versus control; # $p < 0.05$ versus JX; \$ $p < 0.05$ versus α PD-1. ns, not significant. Two-tailed Student's *t*-test was used. Scale bars, 100 μ m.

Figure 4. The efficacy of combination immunotherapy with intratumoral JX and systemic ICIs is not largely affected by treatment schedule.

Mice were s.c. implanted with Renca tumor cells and treated with JX plus ICIs on various schedules.

(A) Diagram depicting various treatment schedules. Arrows indicate treatment with either intratumoral delivery of JX (red) or systemic delivery of ICIs (blue).

(B) Comparison of tumor growth in mice treated with JX and α PD-1 using different treatment schedules. Mean and individual tumor growth curves over time.

(C) Representative flow cytometric plot showing tumor-infiltrating CD8⁺ and CD4⁺ T cell fractions.

(D) Comparisons of absolute numbers of CD8⁺, CD4⁺, CD8⁺ICOS⁺, and CD8⁺GzB⁺ cells per gram of tumors.

Pooled data from two experiments with 7 animals per group. Values are mean \pm SEM. * $p < 0.05$ versus control. ns, not significant. Two-tailed Student's *t*-test was used.

Figure 5. The triple combination of JX and α PD-1 and α CTLA-4 induces profound tumor regression and provides a long-term survival benefit in kidney cancer.

Mice were s.c. implanted with Renca tumors and treated with or without JX and immune checkpoint blockades for PD-1 and CTLA-4 on the indicated days (arrows).

(A) Comparisons of tumor growth. Mean and individual tumor growth curves over time. Pooled data from two experiments with 8 animals per group. * $p < 0.05$ versus control; # $p < 0.05$ versus JX; \$ $p < 0.05$ versus α PD-1+ α CTLA-4. ns, not significant. Two-tailed Student's *t*-test was used.

(B) Waterfall plot showing the maximal percent changes from baseline in tumor size.

(C) Comparison of tumor size after injection of Renca or CT26 tumor cells into mice with complete tumor regression or into naïve mice.

(D) Kaplan-Meier plot for overall survival. $n = 8-11$ for each group. Log-rank test was used.

Figure 6. The triple combination therapy delays tumor growth and metastasis in a spontaneous breast cancer model.

Growth of spontaneous mammary tumors of *MMTV-PyMT* mice was analyzed starting from 9 weeks after birth. Samples were harvested 13 weeks after birth.

(A) Diagram depicting the treatment schedule. Arrows indicate treatment with or without intratumoral delivery of JX and systemic delivery of α PD-1 (P) and α CTLA-4 (C).

(B) Representative image showing gross appearance of tumors. Dotted-line circles demarcate palpable mammary tumor nodules.

(C) Comparison of total tumor burden. Tumor burden was calculated by summing the volume of every tumor nodules per mouse.

(D) Comparison of number of palpable tumor nodules.

(E) Comparison of volume of each tumor nodule. Each tumor nodule in *MMTV-PyMT* mice is plotted as an individual dot.

(F) Kaplan-Meier curves for overall survival. Log-rank test was used.

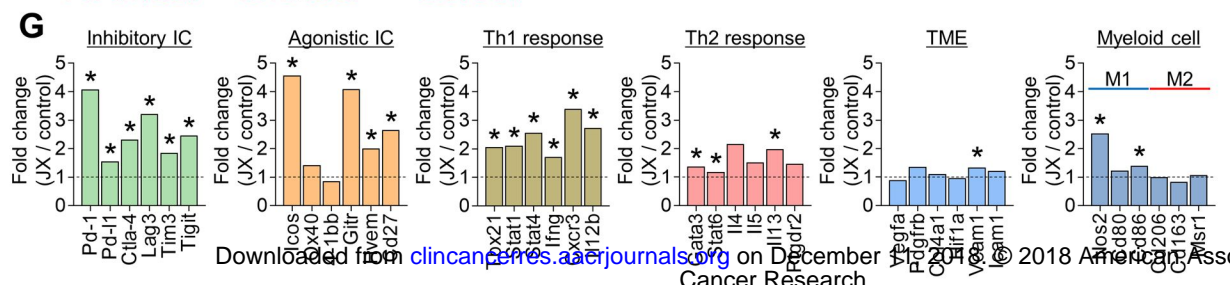
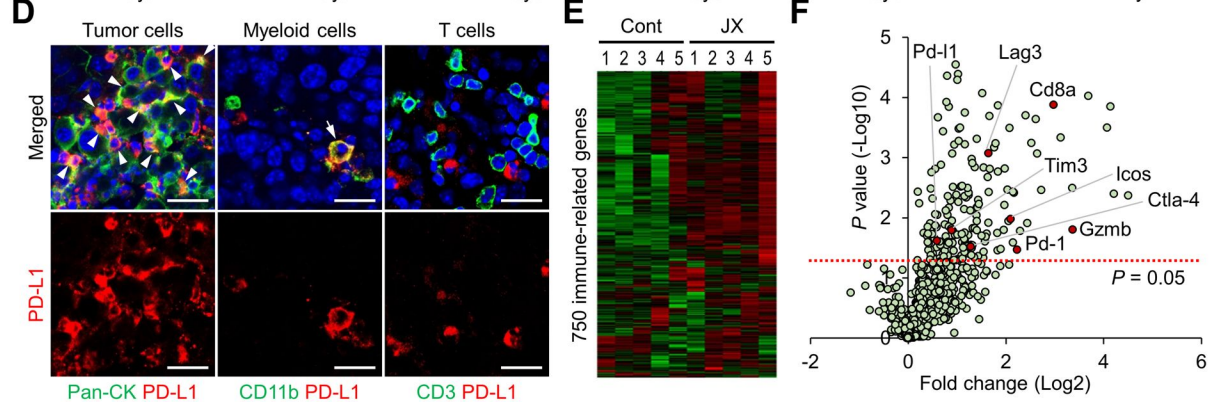
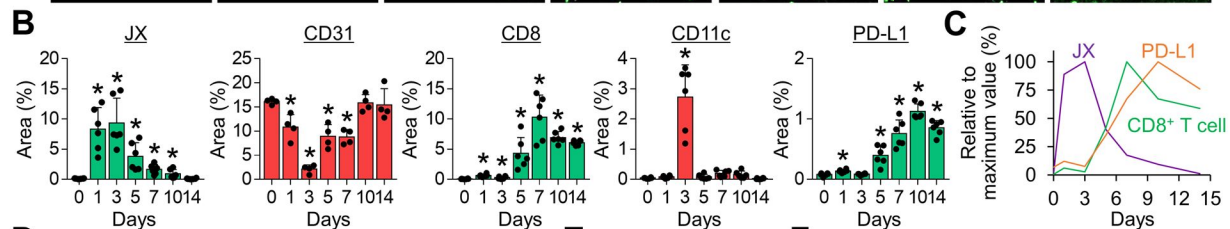
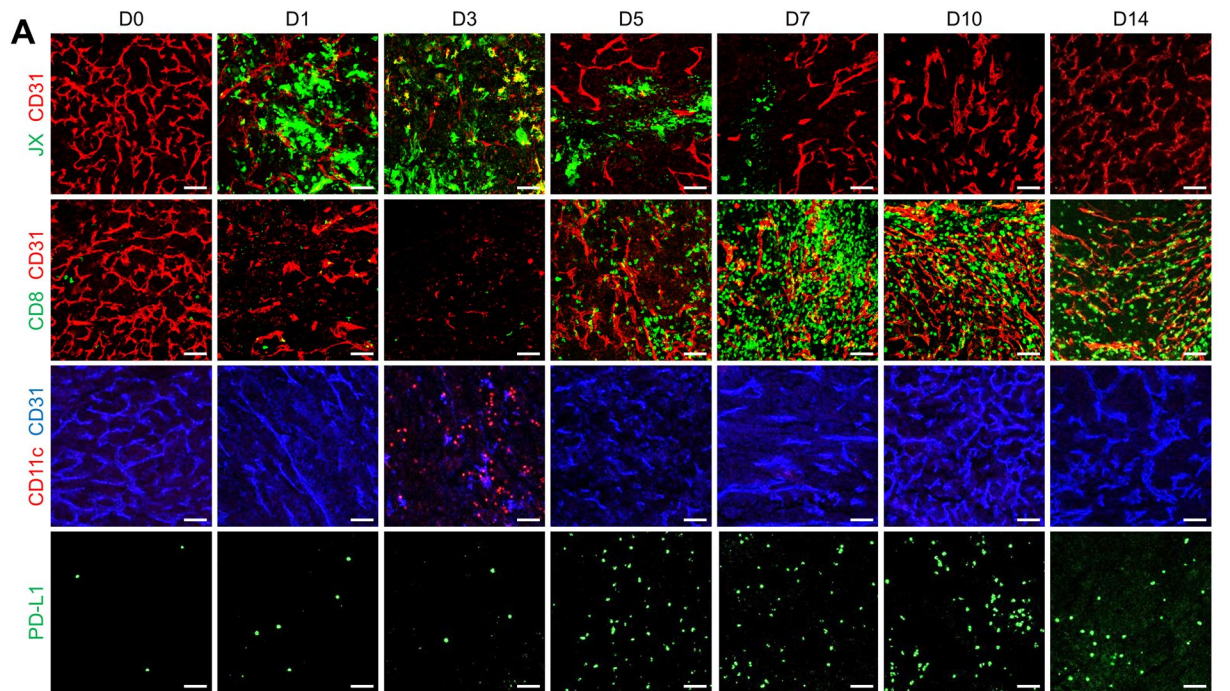
(G) H&E-stained tumor sections showing intratumoral regions. Acinar structures of JX and JX+P+C groups are early, less-invasive lesions (Ea) showing the distinct boundary with the surrounding mammary adipose tissue (Adi). Invasive ductal carcinoma regions (Ca) of Cont and P+C have massively invaded into the surrounding tissue and formed solid sheets of tumor cells with no remaining acinar structure.

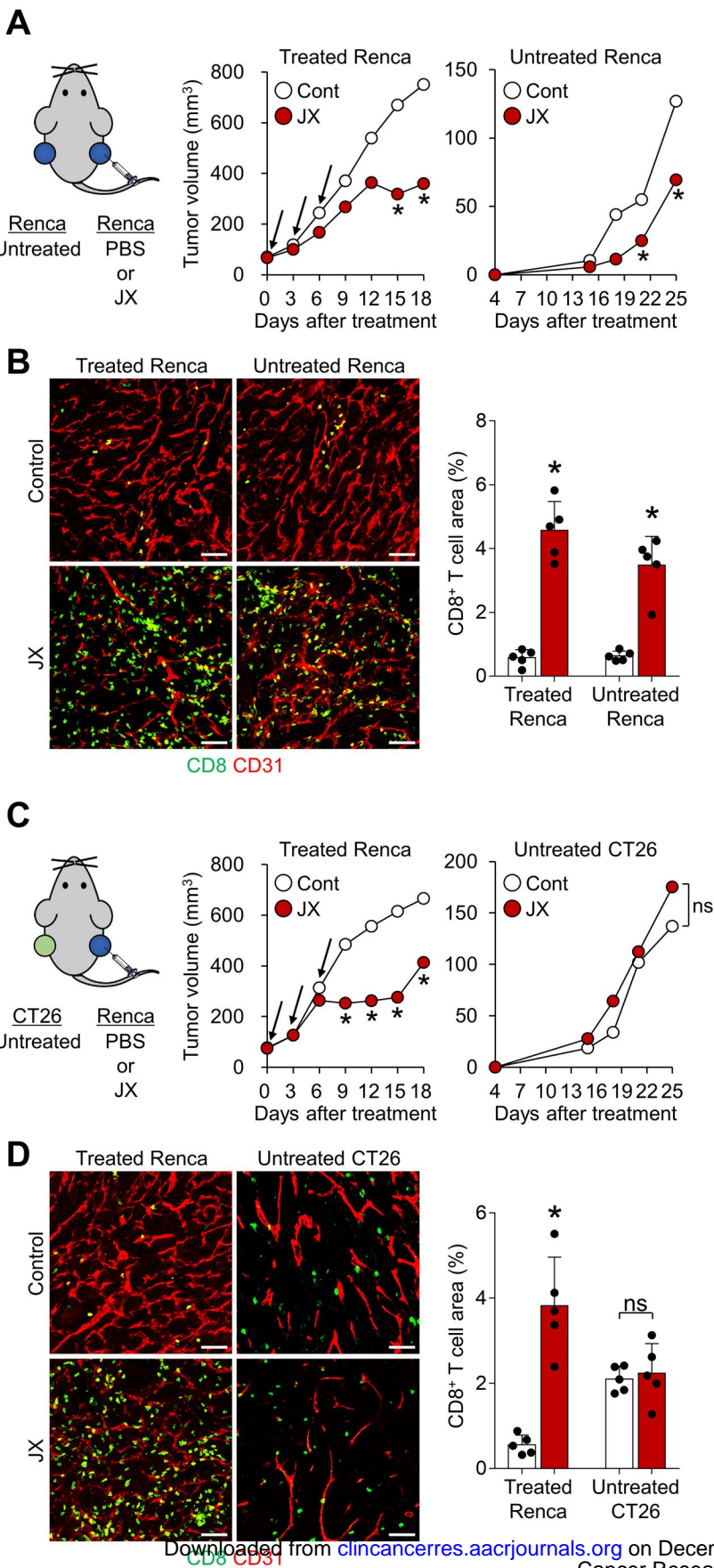
(H) Representative images and comparisons of CD8⁺ T cells and CD31⁺ tumor blood vessels in tumor.

(I) Representative lung sections stained with H&E and comparison of the number of metastatic colonies per lung section. Arrows indicated metastatic foci.

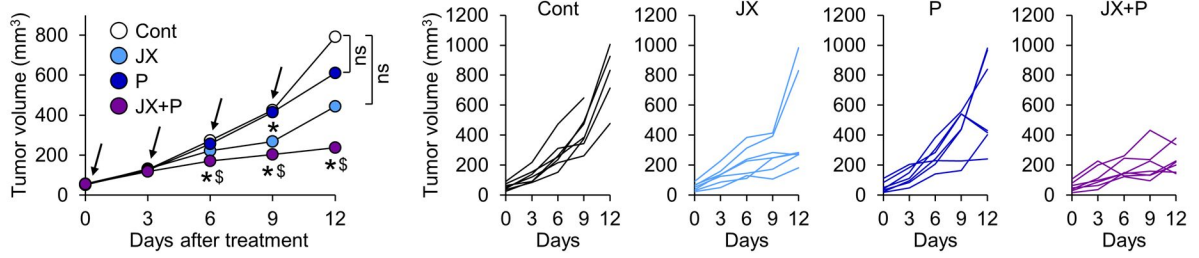
Unless otherwise denoted, n = 8-9 for each group. Values are mean \pm SD. *p < 0.05 versus

control; [#]p < 0.05 versus JX; ^{\$}p < 0.05 versus αPD-1+ αCTLA-4. ns, not significant. Two-tailed Student's *t*-test was used in 6C-E, H, and I. Scale bars, 200 μm.

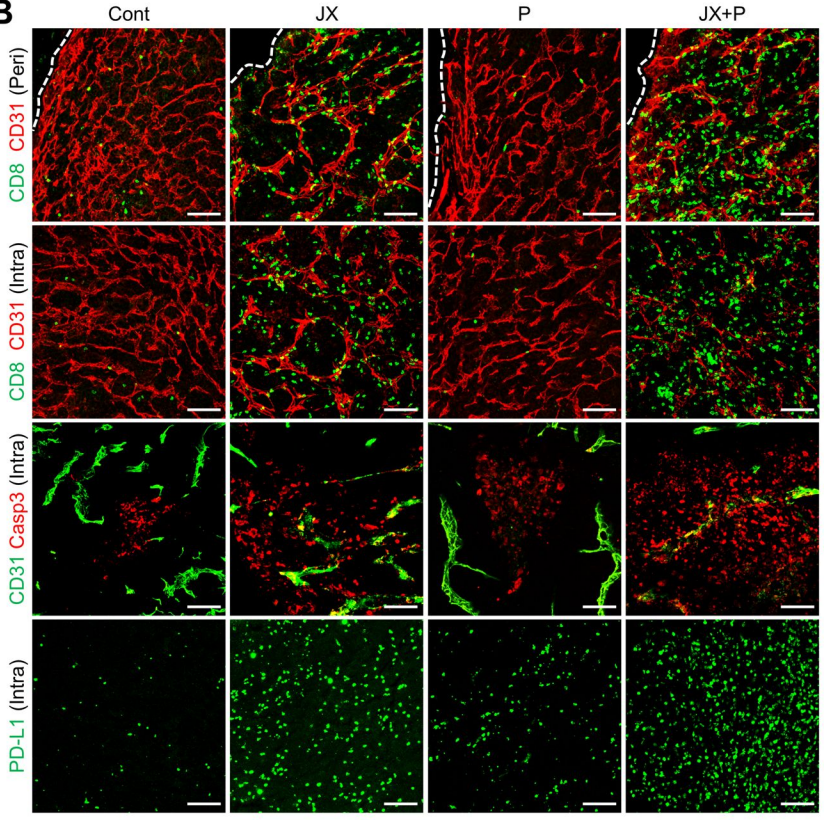




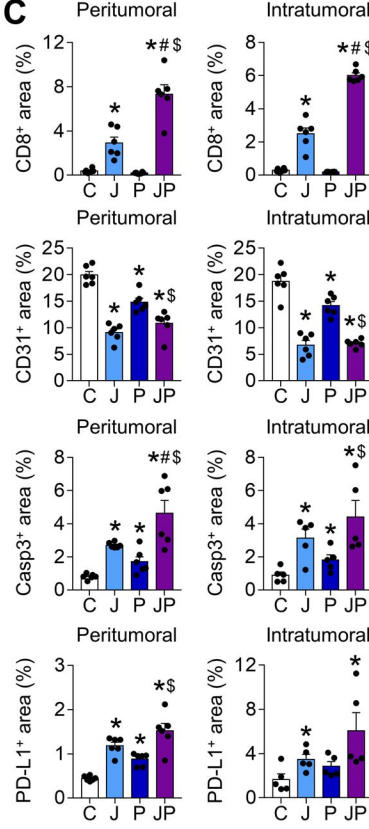
A



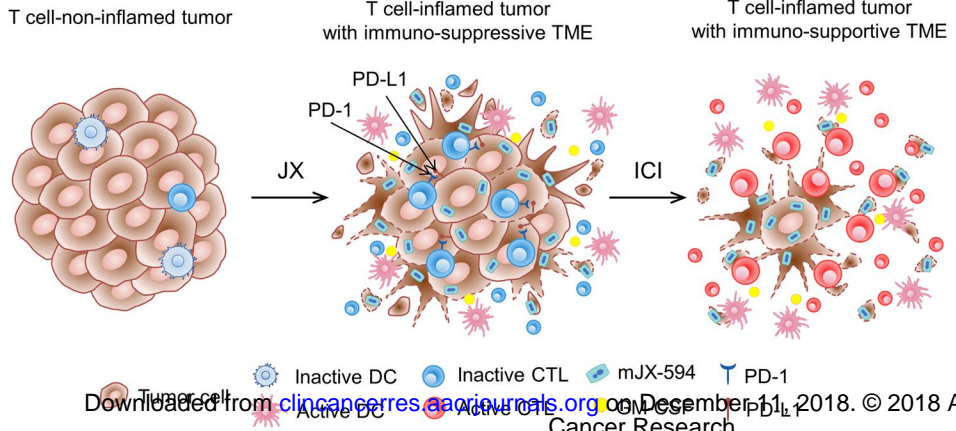
B

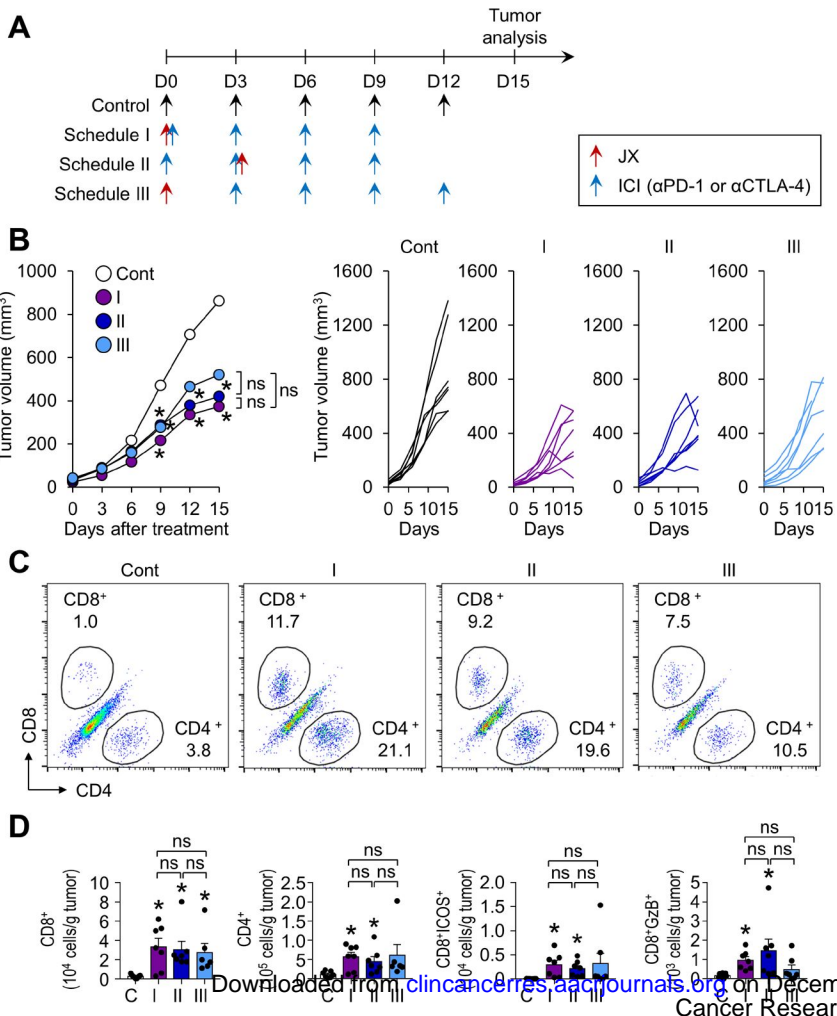


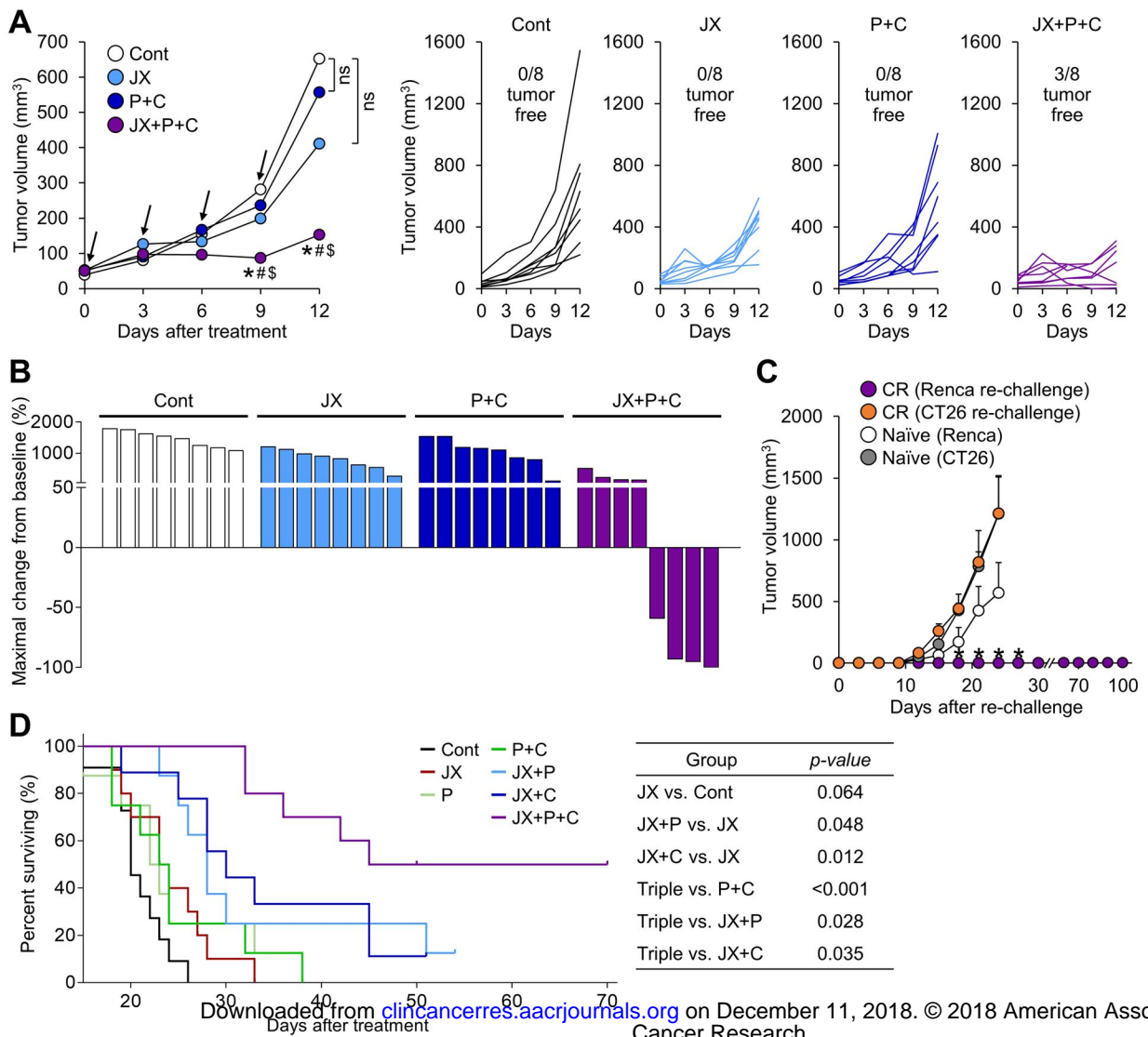
C

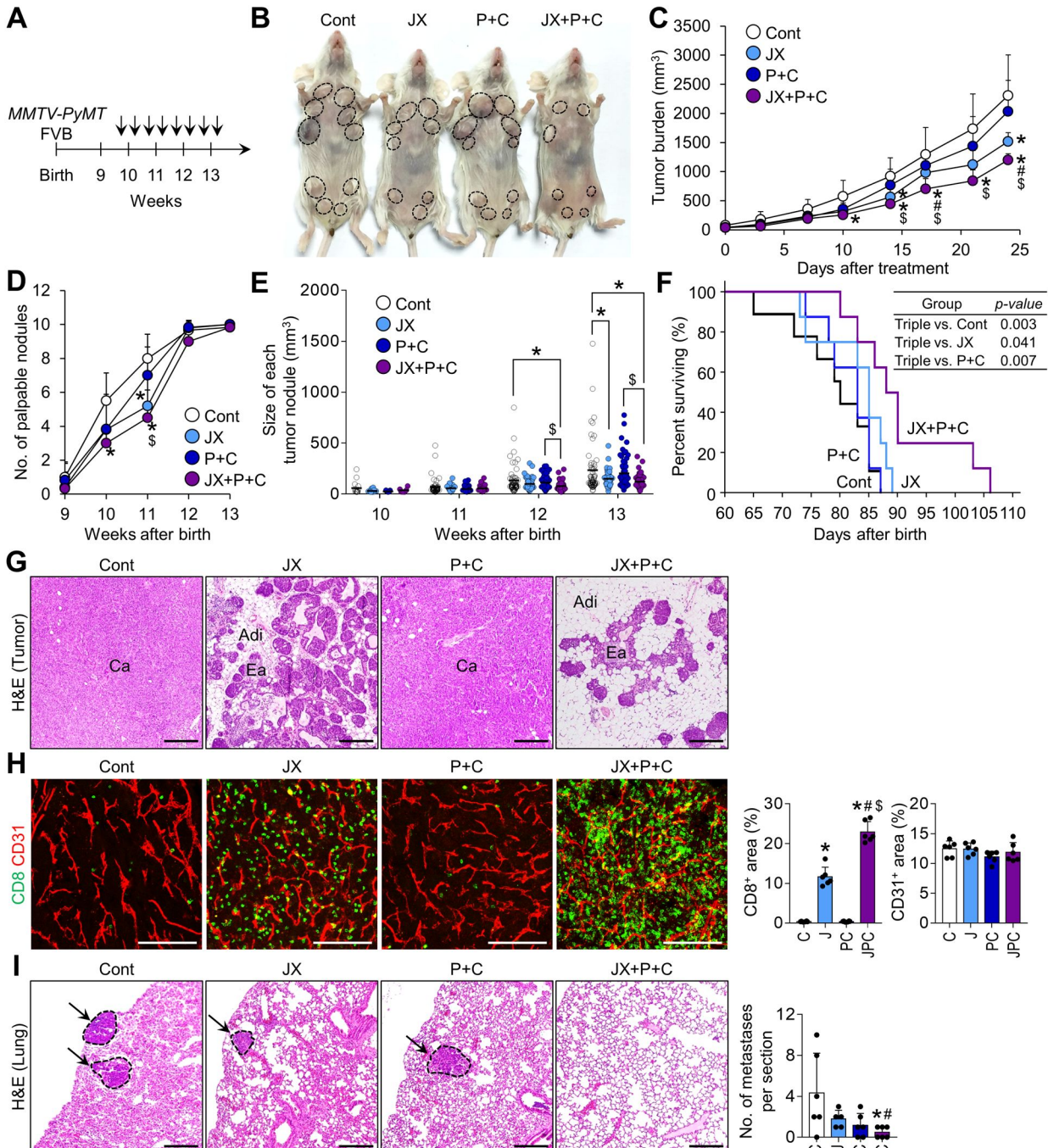


D









Clinical Cancer Research

Tumor microenvironment remodeling by intratumoral oncolytic vaccinia virus enhances the efficacy of immune checkpoint blockade

Hong Jae Chon, Won Suk Lee, Hannah Yang, et al.

Clin Cancer Res Published OnlineFirst December 11, 2018.

Updated version	Access the most recent version of this article at: doi: 10.1158/1078-0432.CCR-18-1932
Supplementary Material	Access the most recent supplemental material at: http://clincancerres.aacrjournals.org/content/suppl/2018/12/11/1078-0432.CCR-18-1932.DC1
Author Manuscript	Author manuscripts have been peer reviewed and accepted for publication but have not yet been edited.

E-mail alerts	Sign up to receive free email-alerts related to this article or journal.
Reprints and Subscriptions	To order reprints of this article or to subscribe to the journal, contact the AACR Publications Department at pubs@aacr.org .
Permissions	To request permission to re-use all or part of this article, use this link http://clincancerres.aacrjournals.org/content/early/2018/12/11/1078-0432.CCR-18-1932 . Click on "Request Permissions" which will take you to the Copyright Clearance Center's (CCC) Rightslink site.